World Academy of Science, Engineering and Technology
International Journal of Materials and Metallurgical Engineering
Vol:12, No:3, 2018

Numerical Modelling of Surface Waves Generated by Low Frequency Electromagnetic Field for Silicon Refinement Process

V. Geza, J. Vencels, G. Zageris, S. Pavlovs

Abstract**—**One of the most perspective methods to produce SoG-Si is refinement via metallurgical route. The most critical part of this route is refinement from boron and phosphorus. Therefore, a new approach could address this problem. We propose an approach of creating surface waves on silicon melt's surface in order to enlarge its area and accelerate removal of boron via chemical reactions and evaporation of phosphorus. A two dimensional numerical model is created which includes coupling of electromagnetic and fluid dynamic simulations with free surface dynamics. First results show behaviour similar to experimental results from literature.

Keywords**—**Numerical modelling, silicon refinement, surface waves, VOF method.

I. Introduction

THE exhaustion of fossil fuel resources, global warming, and increased energy consumption all make finding alternative energy sources important. In terms of environmental impact, solar energy is one of the most perspective and attractive sources. However, development of solar power is limited by the solar power costs in comparison to other power sources. As shown in [1], by 2020 the energy cost for solar power is still expected to be higher than for hydro, onshore wind, geothermal, nuclear and even biomass energy sources. Reduction of solar cell production costs is necessary for this technology to develop, and one solution is to reduce the cost of raw materials like polysilicon.

In 2013, production of polysilicon constituted approx. 23% of the total solar cell costs [2]. This number can be reduced by lowering energy consumption during solar grade silicon (SoG-Si) production. One of the most efficient ways to produce SoG-Si is the metallurgical route of refining. It consumes about 30 kWh/kgSi (kilowatt-hours per kilogram of silicon) of energy. In comparison, a chemical route such as the Siemens process, which is the most widely used refining process nowadays, consumes more than 70 kWh/kgSi [3]. In 2013, more than 200 000 tons of polysilicon was produced worldwide, which could result in more than an 8 TWh reduction if all of the silicon was produced via the metallurgical route rather than with the Siemens process.

Currently, the polysilicon market is recovering from a crisis, and new technologies that ensure reduction of production costs can give a significant advantage in a competitive SoG-Si market. In April 2017, a three year project was started in University of Latvia on refinement of silicon via the metallurgical route. The main task of this project is increasing the efficiency of silicon refinement from boron and phosphorus with use of advanced electromagnetic impact.

V. Geza, J. Vencels and S. Pavlovs are with the Department of Physics and Mathematics of the University of Latvia, Riga, LV-1002, Latvia.

G. Zageris is with the Department of Physics and Mathematics of the University of Latvia, Riga, LV-1002 (corresponding author, phone: +37129385266; e-mail: girts.zageris@fizmati.lv).

II. Potential for EM Technologies in Silicon Refinement

In many investigations, phosphorus removal is found to be the most challenging task, since the purity threshold (< 1 ppm) is not reached [8]. Although, oxidation and slag refinement is a simple process for removing phosphorus from silicon, it is insufficient to reach the low purity threshold. The most used approach for phosphorus removal is evacuation; it is dependent on free surface area and bulk melt stirring. Refinement enhancement can be achieved by superposing DC and AC magnetic fields [7]. Furthermore, this impact creates a mixing effect in the bulk melt, which is also important for boron removal. In comparison, classical induction stirring can enhance only bulk melt mixing, leaving surface area size unchanged.

Boron removal by oxidizing bubbles was already shown in [4] where significant splashing of silicon was observed, and it was determined that the blowing of oxidizing gas on free surface of the silicon was preferred instead. Also, no attempt was made to adapt electromagnetic stirring for bubble flow control, which was shown to be possible in [5]. Furthermore, high velocity shear in the melt can lead to gas bubble breakup, thus enlarging gas-liquid interface area and increasing boron removal rate.

Another possibility for boron removal could be blowing of oxidizing gas on free surface, which is already well known [6], and with additional creation of surface waves by means of electromagnetic impact, thus creating capillary waves and increasing surface area at least twice. The aforementioned electromagnetic impact technology (superposition of DC and AC fields) can be used for boron evaporation, because it enhances surface area and stirring.

Highest boron refining rates can be achieved with plasma refining, but it has high energy demand. In reactive gas refining, concentration of boron changes according to the first order rate law.

$$ln\left[\frac{C_{B,0}}{C_{B,t}}\right] = k_B \frac{A}{V} t \quad (1)$$

Here C_B – boron concentration with indices after comma indicating time, A is the area of interfacial surface between oxidizing gas and silicon melt, V is the volume of silicon melt, t is time, k_B is boron mass transfer coefficient at the surface, measured in μm/s. k_B is determined experimentally and is dependent on the oxidizing gas supply rate, the type of oxidizing gas and melt temperature. Creation of surface waves would increase the A/V ratio, thus speeding up boron removal. Table I summarizes k_B from literature with different oxidizing gases, gas flow rates and temperatures.

TABLE I
SILICON REFINING FROM BORON AND PHOSPHORUS SUMMARY FROM LITERATURE

Oxidizing gas	Melt tempera-ture T, ºC	Flow rate, Nl/min	k_B, μm/s	Reference
Ar – 97 %, H_2O – 3%	1450	3	7.0	
N_2 – 97 %, H_2O– 3%	1450	3	6.0	[9]
H_2 – 97 %, H_2O– 3%	1450	3	13.0	
H_2 – 24.2 %, Ar – 72.6 %, H_2O– 3.2%	1500	3	4.3	
H_2 – 48.4 %, Ar – 48.4 %, H_2O– 3.2%	1500	3	8.6	[10]
H_2 – 72.6 %, Ar – 24.2 %, H_2O– 3.2%	1500	3	9.2	
H_2 – 97 %, H_2O– 3%	1450	3	13.0	
H_2 – 97 %, H_2O– 3%	1500	2	9.0	[6]
H_2 – 97 %, H_2O– 3%	1500	14	44.6	
Boron / **Phosphorus**	**Melt tempera-ture T, ºC**	**Pressure, Pa**	**k_P, μm/s**	**Reference**
	1500	0.5	2.28	[11]
	1600	0.5	4.93	

Data from Table I show that the most important factor for boron removal is oxidizing gas and its flow rate.

According to [11], the same relation as (1) is applicable for phosphorus removal; literature data is also shown in Table I. For phosphorus, temperature is a more important factor. Another important factor is pressure. According to [12], the phosphorus mass transfer coefficient on the surface of the silicon melt strongly depends on pressure. Above 1 Pa pressure, the transfer rate of phosphorus declines very rapidly. On the other hand, phosphorus mass transfer coefficient reaches an asymptotical value below 0.1 Pa and therefore further decrease in pressure would not be beneficial.

For removal of both boron and phosphorus, surface waves can be used to enlarge surface area and increase refinement rate. However, it is not clear how large the surface enlargement will be and how it will influence boron diffusion in the gas boundary layer. For this purpose, the first step is the creation of a numerical model which can simulate melt's surface waves induced by electromagnetic impact.

III. SIMULATION MODEL

For numerical simulations we use two open-source software packages - the finite element multi-physics simulation code Elmer and computational fluid dynamics code OpenFOAM. Efficient parallel coupling between both codes is done using EOF-Library [13].

Computation scheme is shown in Fig. 1 (a). OpenFOAM (OF) package solves fluid dynamics with free surface using volume of fluid (VOF) method, then computes electrical conductivity of gas-and-melt mixture and sends it to Elmer package. Elmer solves the complex problem for the time-harmonic electromagnetic (EM) field and sends back to OF the complex components of electrical current density and magnetic field density.

Every time the EM field is updated, the amplitudes are computed

$$J_0^i = \sqrt{J_\Im^2 + J_\Re^2}$$
$$B_0^i = \sqrt{B_\Im^2 + B_\Re^2} \quad (2)$$

And the corresponding phases

$$\varphi_J^i = atan2\left(J_\Im^i, J_\Re^i\right)$$
$$\varphi_B^i = atan2\left(B_\Im^i, B_\Re^i\right) \quad (3)$$

for current and magnetic field densities, where i represents x, y and z components, and *atan2* is the arctangent function with two arguments that gives the angle in radians between the x-axis and the specified point. Then, at every OF timestep the Lorentz force is updated

$$F^x = exp\left(\frac{-2}{\omega t}\right) \cdot J_0^z cos\left(\varphi_J^z + \omega t\right) \cdot B_0^y cos\left(\varphi_J^y + \omega t\right)$$
$$F^y = -exp\left(\frac{-2}{\omega t}\right) \cdot J_0^z cos\left(\varphi_J^z + \omega t\right) \cdot B_0^x cos\left(\varphi_J^x + \omega t\right) \quad (4)$$
$$F^z = 0$$

where ω is angular frequency. An exponential multiplier provides a smooth increase of the Lorentz force during the first few periods and reduces unwanted splashes at the beginning of simulation.

A 2D axisymmetric problem of mercury with free surface is considered. The mercury tank is surrounded by an inductor, which creates an alternating magnetic field; see Fig. 1 (b) for illustration. A similar device and experiment was described in [14]. This mercury experiment is only used for model validation purposes. In this model, mercury properties were

set in the melt domain - electrical conductivity σ_{melt}=1.04·10^6 S/m, kinematic viscosity ν_{melt} = 1.14·10^{-7} m^2/s, density ρ = 13534 kg/m^3, surface tension γ = 0.5 N/m and contact angle θ = 90°. The inductor has homogeneous current distribution with density J_{ampl} = 6.5·10^6 A/m^2 and frequency f = 14 Hz. Turbulence model k-ε is used, and maximal Courant number is set to 0.4. The transient simulation reaches flow time 4 sec.

The computational mesh for OF has 31k cells, mesh for Elmer has 35k elements. We used a very fine mesh with size 0.35mm in the region where surface can be present during simulation; see Fig. 1 (c).

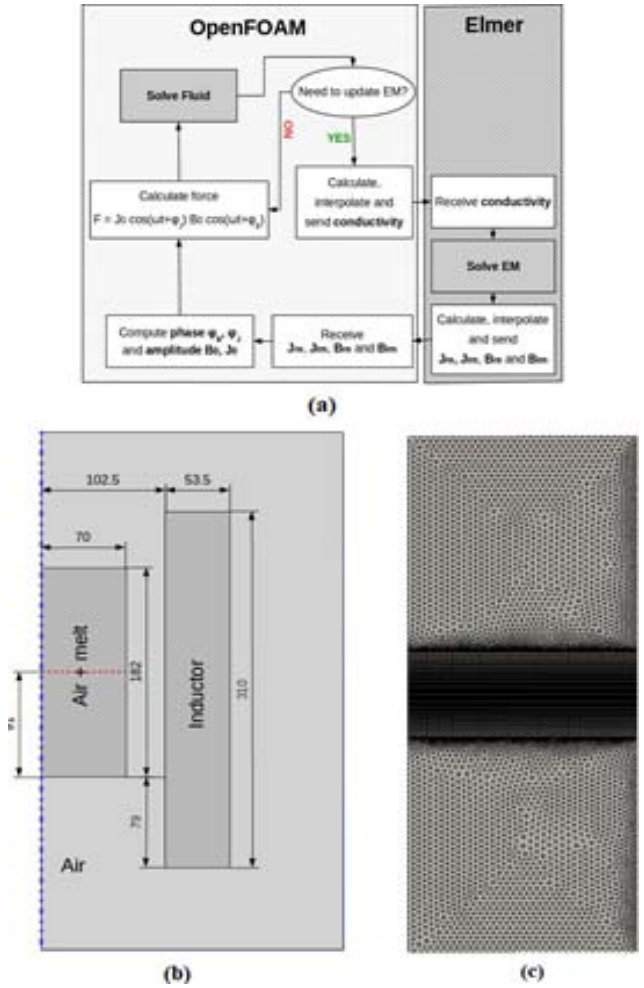

Fig. 1 Computational scheme for coupled OF and Elmer simulation (a). Schematic drawing for 2D axisymmetric model (b), where vertical dashed line is symmetry axis and horizontal dashed line is melt's initial filling level. All sizes given in millimeters. OF fluid dynamics mesh (c)

IV. Results

The turbulent flow (Re ≈1.5·10^5) inside the mercury vessel has two toroidal vortices similar to a classical induction crucible. But in the considered case, the slow change of the EM force causes creation of surface waves near the outer wall, and subsequent propagation of waves radially inward. Fig. 2 (a) shows the velocity field in the melt and air. The velocity vectors in this figure that have also vertical component only indicate that melt surface is moving and there is no net melt mass moving through the interface.

Frequency analysis of local melt height in three points (x=0 on axis, x=35mm, and x= 70mm near wall) shows several peaks. The peak at 28 Hz relates to the frequency of the EM force, which is double the EM field frequency. There is a 14 Hz peak close to the wall, in simulation results it was observed that 28 Hz force frequency creates two small waves that fuse into one wave.

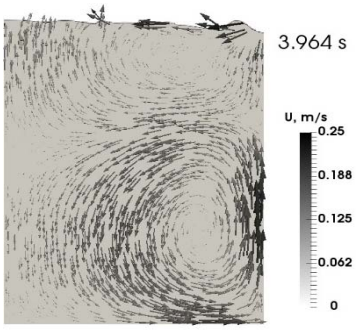

(a)

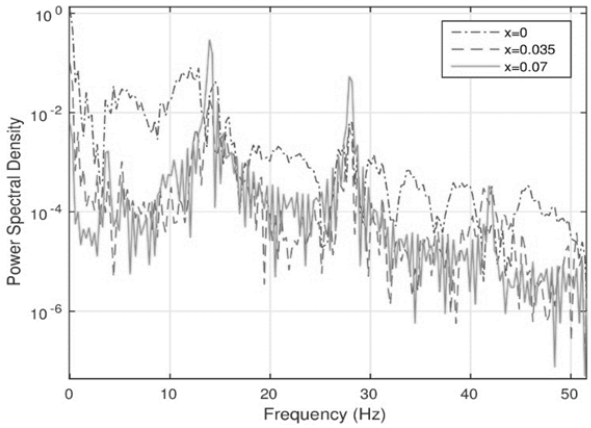

(b)

Fig. 2 Melt's surface shape and velocity distribution at 3.964 s (a) and wave frequencies at three different radial coordinates (b)

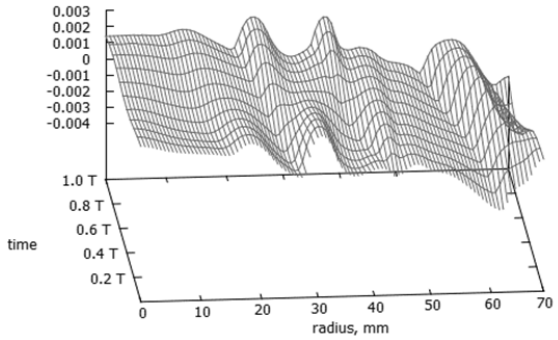

Fig. 3 Melt surface height radial dependence in time. Vertical axis shows melt height in meters

The time dependence for the surface shape of melt can be

seen in Fig. 3. It was observed that waves on the surface are not regular during the first two seconds. At first, waves are travelling radially toward the center of the crucible, and when waves reach the center, waves travelling away from the center appear. After two seconds, first standing waves start to appear when oppositely travelling waves interfere. Obtained values of wavelength λ do not correspond to experimental data from literature [14], in current simulation there are 5-6 λ that fit into one radius, while there are 10 λ in the experiment. In the current simulation, standing waves are established after initial wave development has passed. Standing waves are also found for a similar configuration as described in [15].

V. Conclusions and Outlook

The numerical model we developed showed that standing waves are formed on melt's surface after first two seconds and that these waves are formed by travelling waves moving radially in opposite directions. There are very few references on numerical modelling of such problems and therefore these promising results are important steps towards better understanding and capturing EM induced capillary waves on liquid metal surface. However, detailed behaviour of surface is not captured. There is discrepancy with literature for results of the shape of waves, and no sufficient experimental data on wave amplitudes exist. There are two possible ways to achieve more detailed results.

The first option is the adaptation of the existing model by means of adjusting time and space resolutions. Temporal resolution restrictions are caused by capillary waves. Advanced numerical techniques can also be used to diminish numerical artefacts.

The second option is implementation of other surface capture techniques, different than VOF. One possible approach is the height function method.

Acknowledgment

This work was funded by European Regional Development Fund under contract "Refinement of metallurgical grade silicon using smart refinement technologies" (No. 1.1.1.1/16/A/097).

References

[1] "U. S. Energy Information Administration (EIA) – Source": www.eia.gov. Retrieved 2016-06-07.

[2] "GTM Research": www.greentechmedia.com/articles/read/solar-cost-reduction-drivers-in-2017. Retrieved 2016-06-06.

[3] Fu, R., James, T. L., Woodhouse, M.: *Measurements of polysilicon for the photovoltaic industry: market competition and manufacturing competitiveness*. IEEE Journal of Photovoltaics, Vol. 5, 2015, No. 2, pp. 515–524.

[4] Sortland, Ø.S.: *Boron removal from silicon by steam and hydrogen. PhD Thesis*. Norwegian University of Science and Technology, Trondheim, 2015, 268 p.

[5] Sand, U., Yang, H., Eriksson, J-E., Bel Fdhila R.: *Numerical and experimental study on fluid dynamic features of combined gas and electromagnetic stirring in ladle furnace*. Steel Research International, Vol. 80, 2009, No. 6, pp. 441–449.

[6] Sortland, Ø. S., Tangstad, M.: *Boron removal from silicon melts by H_2O/H_2 gas blowing: mass transfer in gas and melt.* Metallurgical and Materials Transactions E. Vol. 1, 2014, No. 3, pp 211–225.

[7] Bojarevičs, A., Beinerts, T., Grants, I., Kaldre, I., Šivars, A., Gerbeth, G., Gelfgat Yu.: *Effect of superimposed DC magnetic field on an AC induction semi-levitated molten copper droplet*. Magnetohydrodynamics, Vol. 51, 2015, No. 3, pp. 437–444.

[8] Khattak, C.P., Joyce, D.B., Schmid, F.: *A simple process to remove boron from metallurgical grade silicon*. Solar Energy Materials and Solar Cells, Vol. 74, 2002, No. 1, pp. 77–89.

[9] Safarian, J., Thang, K., Hildal, K., Tranell, G.: *Boron removal from silicon by humidified gases.* Metallurgical Transactions E, Vol. 1E, 2014, pp. 41–47.

[10] Nordstrand, E. F., Tangstad, M.: *Removal of boron by moist hydrogen gas*. Metallurgical Material Transactions B, Vol. 43, 2012, No. 4, pp. 814–822.

[11] Safarian, J., Tangstad, M.: *Kinetics and mechanism of phosphorus removal from silicon in vacumm induction refining*. High Temperature Material Processing, Vol. 31, 2012, pp. 73–81.

[12] Zheng, S., Safarian, J., Seongho, S., Sungwook, K., Tangstad, M., Luo, X.: *Elimination of phosphorus vaporizing from molten silicon at finite reduced pressure*. Transactions of nonferrous metals society of China. Metals, vol. 21, 2011, pp. 697–702.

[13] Vencels, J., Jakovics, A., Geza, V., Scepanskis, M.: *EOF Library: Open-Source Elmer and OpenFOAM Coupler for Simulation of MHD with Free Surface*. XVIII International UIE-Congress "Electrotechnologies for Material Processing", 2017, pp. 312–317.

[14] Saadi, B., Bojarevics, A., Fautrelle, Y., Etay, J.: *Electromagnetic control of mass transfer at liquid/liquid interfaces (in French)*. Récents Progrè en Génie des Procédés (ISBN 2-910239-66-7), Paris, France, No. 92, 2005.

[15] Fautrelle, Y., Sneyd, A.D.: *Surface waves created by low-frequency magnetic fields*. Europeand Journal of Mechanics B/Fluids, Vol. 24, 2005. pp. 91–112.